Available online at www.sciencedirect.com

SciVerse ScienceDirect

Proceedings of the Combustion Institute 34 (2013) 1401–1409

Proceedings of the Combustion Institute

www.elsevier.com/locate/proci

Streamline segment analysis of turbulent premixed flames

Lipo Wang [a,c,*], Nilanjan Chakraborty [b], Jian Zhang [c]

[a] UM-SJTU Joint Institute, Shanghai JiaoTong University, Shanghai 200240, China
[b] School of Mechanical and Systems Engineering, Newcastle University, Newcastle-Upon-Tyne NE1 7RU, United Kingdom
[c] LNM, Institute of Mechanics, Chinese Academy of Sciences, Beijing 100080, China

Available online 20 July 2012

Abstract

In this study the streamline segment analysis has been carried out for turbulent premixed flames in order to analyze the statistical properties of the flame surface, which are associated with the nearby extremal points. The analysis is based on a DNS database of freely propagating turbulent premixed flames with a wide variation of turbulence and combustion parameters, spanning different combustion regimes. Typically a streamline segment can be characterized by its curve length l and the difference of the velocity magnitude at two extremal points Δu. It has been found that an expression for the probability density function (PDF) of l, originally developed for non-reacting turbulent flows, remains valid for turbulent premixed flames in the thin reaction zones regime at high values of turbulent Reynolds number. However, the agreement between the theoretical prediction and the PDF of l obtained from DNS data worsens with decreasing turbulent Reynolds number, as well as in the corrugated flamelets regime. The joint PDFs between l and Δu and between l and $\Delta \rho u$ have been analyzed in detail, and it has been found that turbulence intensity, heat release parameter and the regime of combustion have significant effects on these joint PDFs. Detailed explanations have been provided for the observed differences in the topological behaviors of the streamline segment statistics in response to the combustion kinematics and dynamics.

Keywords: Turbulent premixed flame; Streamline segment analysis; Direct numerical simulation; Flame topology

1. Introduction

The statistical properties of flame surface are of central importance in the flamelet based modeling of premixed turbulent combustion where the reaction zone retains its quasi-laminar structure [1]. The kinematic and dynamic behaviors of flamelets are related to fluid dynamics and the flame topology [2]. The fluid-dynamical effects are often expressed in terms of the local strain rates, whereas the flame topology can be characterized by various parameters, among which the curvature along principal directions is of major significance. There is a large body of the literature on the strain rate and curvature effects on flames [1,3–11]. It has been shown in several previous studies [1,12,7–11] that flame curvature significantly affects the local heat transfer rate, which in turn alters the local flame speed from its planar laminar value. Consequently these curvature

* Corresponding author at: UM-SJTU Joint Institute, Shanghai JiaoTong University, Shanghai 200240, China. Fax: +86 21 3420 6525.
E-mail address: lipo.wang@sjtu.edu.cn (L. Wang).

1540-7489/$ - see front matter © 2012 The Combustion Institute. Published by Elsevier Inc. All rights reserved.
http://dx.doi.org/10.1016/j.proci.2012.06.142

effects appear in the level-set (i.e. G-equation) and the flame surface density (FSD) transport equations, and the corresponding turbulent combustion models [1,13,14]. Moreover, several previous experimental [15] and numerical studies [15,16,7–11] reported a negative correlation between the tangential strain rate and curvature in turbulent premixed flames.

To investigate turbulent combustion as a field phenomenon, it is meaningful to address the geometrical features quantitatively, which is relatively scarce in the existing literature. For example, the vortex tube structure in turbulent flows has been extensively studied; however, the exact definition of vortex tube is yet to be found and thus results thereof are at the best illustrative. Wang and Peters [17] have posited that each spatial point in a scalar field can be associated with a trajectory, along which the scalar magnitude changes monotonically in the local scalar gradient direction between a pair of local maximal and minimal points, where the scalar gradient assumes a zero value. Wang [18] has recently put forward a similar approach known as the streamline segment analysis to analyze the turbulent velocity field statistics. In this analysis, each spatial point can be associated with a streamline segment, along which the velocity magnitude increases (decreases) monotonically in the direction of the local velocity vector between the locations corresponding to the local minimal (maximal) to local maximal (minimal) values of velocity magnitude, where the gradient of velocity magnitude vanishes (see Fig. 2a of Ref. [18]). Interested readers are referred to Refs. [17,18] for further details on the streamline-segment analysis and the significance of extremal points in turbulent flows. In this paper the streamline segment analysis is used to analyze some statistical and geometrical properties associated with extremal points across the flame surface for a better understanding of turbulence combustion. Although significant advances have been made in flame measurements with valuable phenomenological observations [19,20], experimentation is still incapable of providing detailed time-resolved 3D flow fields and flame topology. Thus three-dimensional direct numerical simulations (DNS) have been used for the present streamline segment analysis in turbulent premixed flames. Detailed physical explanations are provided for the observed behaviors. The statistical properties of the velocity magnitude difference between the extremal points across the flame surface are informative for modeling of turbulent scalar flux, particularly in the context of large eddy simulations [21,22].

2. DNS implementation

DNS of turbulent combustion should account for both three-dimensionality of turbulence and detailed chemical structure of the flame. However, the computational cost of addressing both aspects remains prohibitive [23] for a detailed parametric analysis, as carried out in the present study. Thus, here, the chemical mechanism is simplified using a single-step Arrhenius type irreversible chemistry. In the context of simplified chemistry, the species field is uniquely represented by a reaction progress variable c, which is defined here in terms of non-dimensional temperature as $c = (T - T_0)/(T_{ad} - T_0)$ where T_{ad}, T_0 and T are the adiabatic flame and unburned gas and instantaneous temperatures, respectively.

A DNS database consisting of eight freely propagating statistically planar turbulent premixed flames, labeled as $A - H$, has been investigated here. Case A is taken from a widely used DNS database [24] whereas other cases are simulated using a well-proven compressible DNS code known as SENGA [25]. The simulation domain in all cases is taken to be a rectangular parallelopiped where the x_1 direction is aligned with the direction of mean flame propagation. For cases $B - H$ a 10th-order central difference scheme is used for internal grid points and the order of differentiation gradually decreases to a one-sided 2nd order scheme near non-periodic boundaries. For case A a 6th-order central difference scheme is used in the x_1 direction, while spectral spatial differentiation is applied for transverse directions. The time-advancement for all the viscous/diffusive terms in case A is carried out using an implicit solver, whereas a 3rd-order Runge–Kutta method is used for the reaction rate and convection terms in case A and all the terms in cases $B - H$. For case A (cases $B - H$) the domain boundaries in the x_1 direction are taken to be turbulent inlet and outlet (partially non-reflecting), whereas transverse boundaries are considered to be periodic. The domain and grid sizes for case A are $35.7\delta_{th} \times 44.9\delta_{th} \times 44.9\delta_{th}$ and $261 \times 128 \times 128$, respectively; for cases $B - C$ are $24.1\delta_{th} \times 24.1\delta_{th} \times 24.1\delta_{th}$ and $230 \times 230 \times 230$, respectively; for cases $D - H$ are $36.6\delta_{th} \times 24.1\delta_{th} \times 24.1\delta_{th}$ and $345 \times 230 \times 230$, respectively. The grid spacing is determined by the resolution of the flame structure. About 10 grid points are kept within the thermal flame thickness $\delta_{th} = (T_{ad} - T_0)/\max|\nabla T|_L$, where the subscript L refers to the unstrained planar laminar flame quantities.

Table 1 lists the initial values of the root-mean-square turbulent velocity fluctuation evaluated over the whole domain normalized by the planar unstrained laminar burning velocity u'/S_L, and integral length scale to flame thickness ratio Λ/δ_{th}, along with the values of Damköhler number $Da = \Lambda S_L/(u'\delta_{th})$, Karlovitz number $Ka = (u'/S_L)^{3/2}(\Lambda/\delta_{th})^{-1/2}$, turbulent Reynolds number $Re_t = \rho_0 u'\Lambda/\mu_0$ and heat release parameter $\tau = (T_{ad} - T_0)/T_0$, where ρ_0 and μ_0 are the unburned gas density and viscosity, respectively.

Table 1
Characteristic parameters of DNS.

Case	u'/S_L	Λ/δ_{th}	τ	Re_t	Da	Ka
A	1.41	9.64	2.3	56.70	6.84	0.54
B	7.50	2.45	3.0	46.86	0.33	13.12
C	7.50	2.45	4.5	46.86	0.33	13.12
D	5.00	1.67	4.5	22.00	0.33	8.67
E	6.25	1.44	4.5	23.50	0.23	13.00
F	7.50	2.50	4.5	47.85	0.33	13.00
G	9.00	4.31	4.5	100.00	0.48	13.00
H	11.25	3.75	4.5	110.00	0.33	19.50

Standard values are taken for the Prandtl number $Pr = 0.7$, ratio of specific heats $\gamma = C_p/C_v = 1.4$ and the Zel'dovich number $\beta = T_{ac}(T_{ad} - T_0)/T_{ad}^2 = 6.0$ where T_{ac} is the activation temperature. The Lewis number Le is considered to be unity for all cases. The values of heat release parameter τ, Zel'dovich number β and Lewis number Le characterize the equivalence ratio of premixed flames. The values of β and Le used here are characteristic of a stoichiometric methane–air flame. The value of τ depends on the extent of preheating. The Mach number based on S_L and acoustic speed in the unburned gas a_0 is taken to be 0.014 (i.e. $S_L/a_0 = 0.014$) for all cases. The thermo-physical properties such as viscosity, thermal conductivity, density-weighted mass diffusivity are taken to be constant and independent of temperature. As single-step Arrhenius type chemistry captures the qualitative features of flame propagation [7–11], and flame–turbulence interaction is primarily characterized by the processes taking place in the preheat zone, the assumptions related to simplified transport do not alter the qualitative nature of the statistics presented here.

Case A represents the corrugated flamelets (CF) regime combustion whereas other cases represent the thin reaction zones (TRZ) regime combustion [1]. Among the cases listed in Table 1, case A differs from others in having a much smaller u'/S_L, heat release rate τ and the Karlovitz number Ka. Cases B and C are almost identical, but only differ in terms of τ. Cases $D - H$ have different turbulent Reynolds numbers where the change in Re_t is brought about by modifying Ka or Da independently of each other, as Re_t scales as $Re_t \sim Da^2Ka^2$ [1]. It is worth noting that the range of Re_t for cases $D - H$ remains comparable to that of a previous laboratory-scale experiment [26].

In all cases the flame–turbulence interaction takes place under decaying turbulence. The simulation in case A was run for about 4 initial eddy turn over times ($t_{sim} = 4.0t_f = 4\Lambda/u'$), whereas simulations were run for a time equal to $2.0t_f$ in case G; $3.0t_f$ in cases B, C, D, F and H; and $4.34t_f$ in case E. All the simulation times remain either greater than (case A) or equal to (cases $B - H$) one chemical time scale $t_{chem} = \delta_{th}/S_L$ and these simulation times are comparable to several previous studies [27–30]. The values of u'/S_L decreased by about 52%, 50%, 50%, 45%, 55%, 40%, 25% and 32% of their initial values in cases $A - H$, respectively, at the time when statistics were extracted. By this time, the values of Λ/δ_{th} have increased from their initial values by a factor of about 1.10, 1.7, 1.5–2.25 for cases A, $B - C$ and $D - H$, respectively, but there are still enough turbulent eddies on each side of the computational domain. Moreover, the global turbulent kinetic energy and turbulent flame speed were not changing rapidly with time when the statistics were extracted, which was demonstrated in Fig. 1 of Ref. [32]. Interested readers are referred to Refs. [24,31,32] for more details on the DNS data and the flow conditions when the statistics were extracted.

3. Results and analysis

Unlike analyzing the non-reactive cases where the entire flow field has been taken into consideration [17,18], in the present work, only the quantities related to the flame surface are analyzed. For the present thermo-chemistry, the maximum reaction rate magnitude takes place close to $c = 0.8$, as demonstrated earlier [7,10], and thus the $c = 0.8$ isosurface is considered to be the flame surface. The attention here will mainly be focussed on the statistics related to the geometrical structures of the flame surface. As shown in Fig. 1, for any point on the flame surface, the corresponding streamline segment (SS) is defined as the part of the streamline bound by the two adjacent local extremal points (one maximal in red and one minimal in blue) of the velocity magnitude. Therefore within a streamline segment the velocity magnitude changes monotonously from u_s at the one end to u_e at the other along the direction of velocity vector. The curve length l of the segment and $\Delta u = u_e - u_s$ can be taken to be the characteristic parameters to describe the streamline segments, by which turbulence can be described in a more quantitative manner. According to the sign of Δu (i.e. positive or negative), segments can either be positive or negative. In this paper, the attention

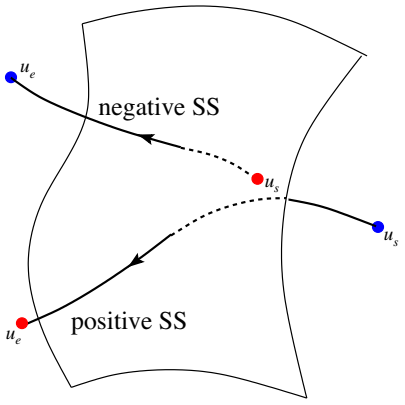

Fig. 1. Illustration of the flame sheet attached with streamline segments (SS), which can be either positive or negative. The red (blue) point represents the maximal (minimal) point of the velocity magnitude. (For interpretation of the references to color in this figure legend, the reader is referred to the web version of this article.)

will be focussed on the relations between the geometric parameters l and Δu, and the flame parameters, such as the surface curvature κ, and θ, the angle between the velocity vector and the flame normal.

3.1. Joint PDF between κ and $cos\theta$

The local curvature is defined as $\kappa = \nabla \cdot (-\nabla c/|\nabla c|)$, where a positive κ indicates a flame surface convex towards the reactants (or the curvature center on the product side), and vice versa. The joint PDF between κ and $\cos\theta$ for case A is shown in Fig. 2a, which exhibits overall skewness towards the negative curvature side. Note that the absolute values of joint PDF for Fig. 2 and subsequent figures are not important for this analysis. The shape of the joint PDF is more important from the point of view of physical arguments. The flame in case A exhibits positively curved bulges and sharp cusps having large values of negative κ (see Fig. 1 in Ref. [10]) due to Huygens propagation, and the Darrius–Landau (DL) instability might also play a role in augmenting this behavior [10]. The joint PDF between κ and $\cos\theta$ for case H is shown in Fig. 2b, which shows a preferential spread towards the positive curvature side. The length scale ratio Λ/δ_{th} does not allow the DL instability to develop for the TRZ regime flames considered here. Moreover, high positive values of displacement speed S_d at highly negative curvature locations due to a strong negative correlation between S_d and κ [12,4–11] prohibit formation of highly negative curved cusps (i.e. $\kappa < 0$). The positive curvature skewness for cases $B - H$ is consistent with previous experimental findings [33] and in accordance with the analysis by Shepherd and Ashurst [2].

The velocity vector aligns closely with the flame normal vector as a result of strong flame normal acceleration in case A due to small value of u'/S_L. However, case H shows that $\cos\theta$ becomes more distributed due to high values of u'/S_L. Stronger perturbation leads to more chaotic turbulent velocity, both along and opposite to the local flame normal, which is reflected in more negative samples of $\cos\theta$.

3.2. Joint PDF between κ and Δu

The joint PDF between κ and Δu for case A is shown in Fig. 3a where Δu assumes predominantly positive values. By contrast, Δu shows significant probability of finding negative values in other cases, as evident from Figs. 3b and 4. A net negative correlation between κ and Δu is observed for the TRZ flames. Thermal expansion (i.e. density drop from unburned reactants to fully burned products) due to heat release acts to increase the velocity magnitude on average towards the burned gas side, in comparison to that in the unburned reactants. By contrast, the decrease of density with temperature rise

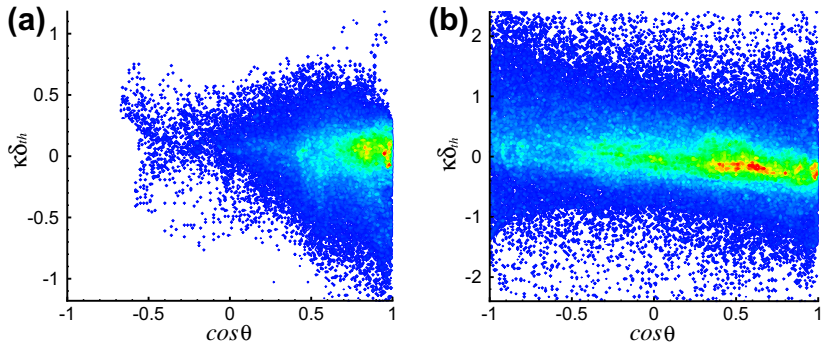

Fig. 2. The joint PDF of $\cos\theta$ and $\kappa \times \delta_{th}$ for (a) case A; (b) case H. The value of joint PDF increases from blue to red region in Fig. 2 and subsequent figures. (For interpretation of the references to color in this figure legend, the reader is referred to the web version of this article.)

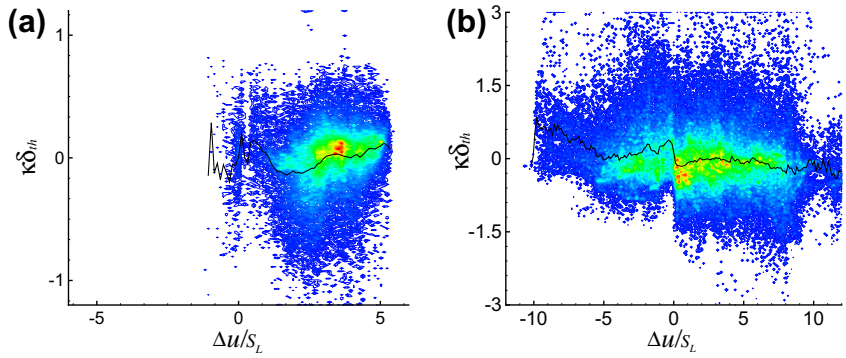

Fig. 3. Joint PDF of $\kappa \times \delta_{th}$ and $\Delta u/S_L$ for (a) case A; (b) case B, where the solid line shows the mean value of κ conditioned on $\Delta u/S_L$ values.

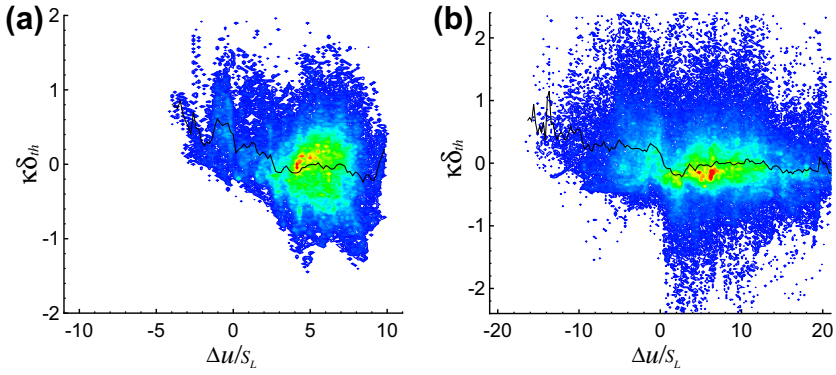

Fig. 4. Same as Fig. 3, but for (a) case *D*; (b) case *H*.

leads to an increase in kinematic viscosity in the burned gas side , which in turn acts to decrease the level of turbulent fluctuation u'. The dilatation rate $\partial u_i/\partial x_i$ is positively correlated with Δu, but negatively correlated with curvature for unity Lewis number flames due to focussing (defocussing) of heat in the negatively (positively) curved zones [9–11]. This curvature dependence is relatively stronger in the TRZ regime than in the CF regime [1]. Therefore Δu negatively correlates with κ for the TRZ cases, while for the CF regime (e.g. case *A*), this negative correlation is much weaker. A predominant probability of finding positive (negative) values of Δu is closely associated with the counter-gradient (gradient) transport of c [21,22,31,31,34,35], which is beyond the scope of this paper and the nature of the turbulent transport for some of the flames considered here can be found elsewhere [21,22,31,34,35].

3.3. The joint PDF between κ and l

The length of streamline segment l gives an indication of the strength of turbulence, i.e. strong turbulent motions disturb streamlines severely so as to make the segments shorter. Figure 5 schematically shows the interaction between turbulent eddies and the preheat zone. This interaction is of central importance for the purpose of understanding the topological features of turbulent premixed flames. Typical eddy sizes in the CF and TRZ regimes of turbulent premixed combustion were estimated in Ref. [1]. In the context of streamline segment analysis, Fig. 5 suggests that such sizes can quantitatively be defined by the mean length of the streamline segments that are locally tangential to the flame surface, i.e. ($l_{\cos\theta=0}$, the conditional mean of l at $\cos\theta = 0$). For case *D* the joint PDF between l and $\cos\theta$ is shown in Fig. 6. The values of $l_{\cos\theta=0}/\delta_{th}$ for cases $A - H$ are 7.77, 3.22, 3.21, 3.67, 4.50, 5.01, 4.92, 4.64, respectively. Comparing these values with Λ/δ_{th} in Table 1 reveals that $l_{\cos\theta=0}$ remains of the same order of the integral length scale Λ in all cases. However, the separation between Λ and the Taylor micro-scale λ remains small for the values of Re_t considered here and thus data for higher values of Re_t will be necessary for more conclusive scaling of $l_{\cos\theta=0}$.

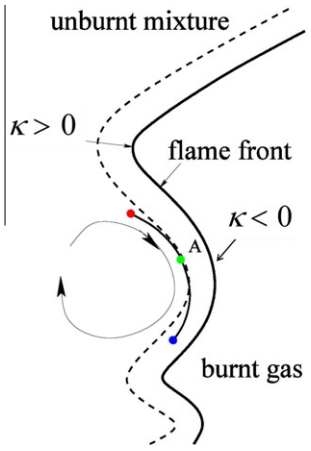

Fig. 5. A schematic diagram describing the interaction of a turbulent eddy with the flame sheet. The eddy size is comparable with the streamline segments (with maximal and minimal velocity magnitude points in red and blue, respectively), which are locally parallel to flames. (For interpretation of the references to color in this figure legend, the reader is referred to the web version of this article.)

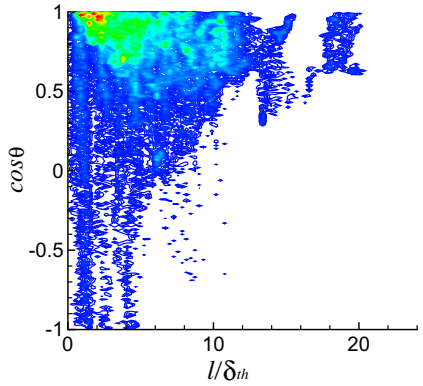

Fig. 6. Joint PDF between l/δ_{th} and cosθ for case D.

3.4. PDF of l/l_m

The PDF of the length of the streamline segments has been analyzed in Ref. [17,18]. A model equation of $P(\tilde{l})$, the PDF of the normalized length $\tilde{l} = l/l_m$, where l_m is the mean of l, is proposed as [17]:

$$\frac{\partial P(\tilde{l},t)}{\partial t}+\frac{\partial}{\partial \tilde{l}}(\tilde{v}(\tilde{l})P(\tilde{l},t))=\Pi\left[\int_0^{\infty}2P(\tilde{l}+\tilde{z},t)d\tilde{z}-\tilde{l}P(\tilde{l},t)\right]$$
$$+8\frac{\partial P(\tilde{l},t)}{\partial \tilde{l}}|_{\tilde{l}=0}\left[\int_0^{\tilde{l}}\frac{\tilde{z}}{\tilde{l}}P(\tilde{l}-\tilde{z},t)P(\tilde{z},t)d\tilde{z}-P(\tilde{l},t)\right]. \quad (1)$$

In Eq. (1), $\tilde{v}(\tilde{l})$ is the drift velocity describing the motion of extremal points relative to each other, and Π is an eigenvalue which can be determined from the PDF's normalization condition. The four terms on the right hand side of Eq. (1) represent generation of $\tilde{l}$ from large scale annihilation, removal of $\tilde{l}$ by perturbation, generation of $\tilde{l}$ from small scale smoothing and removal of $\tilde{l}$ by reconnection, respectively. More detailed mathematical discussion of the above equation can be found in Ref. [17]. Equation (1) is derived based on a general interaction mechanism between turbulent perturbation and molecular diffusion and thus may be suitable for different scenarios. The PDFs of l/l_m extracted from DNS for cases A, B, D and H are compared with the prediction of Eq. (1) in Fig. 7. Both in the linear and log coordinates the predictions of Eq. (1) agree well with the PDFs obtained from DNS data for cases B and H but the agreement is comparatively less satisfactory for cases A and D. This suggests that Eq. (1) predicts $P(l/l_m)$ more satisfactorily for high Re_t flames in the TRZ regime. Although Re_t values are similar in cases A and B, Eq. (1) agrees in a better manner with $P(l/l_m)$ in case B (in comparison to case A) because the effects of heat release are stronger in case A than in case B.

3.5. The joint PDF between l and Δu

The joint PDF between the shape parameters of streamline segments, $P(l,\Delta u)$, has been discussed elsewhere [18] for nonreactive turbulent flows. A typical joint PDF $P(l,\Delta u)$ in non-reacting homogeneous shear turbulence shows strong asymmetry (see Fig. 9 in Ref. [18]). Kinematically positive segments tend to be elongated, while negative segments are compressed, which makes their lengths different on average [18]. A similar tendency can be observed for turbulent premixed flames, in Fig. 8 for case A and B and in Fig. 9 for D and H as well. However, the negative Δu branch in case A almost disappears but this

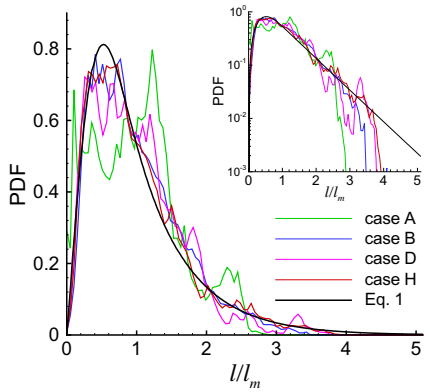

Fig. 7. PDF of the normalized length l/l_m for different cases, compared with the solution obtained from Eq. Eq. (1).

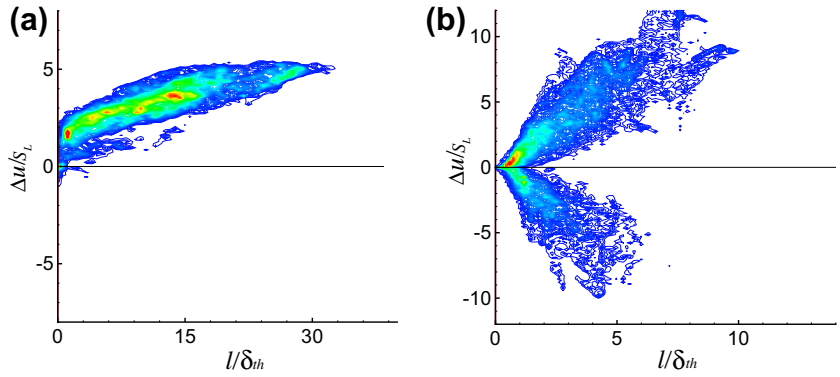

Fig. 8. Joint PDF between l/δ_{th} and $\Delta u/S_L$ for (a) case A; (b) case B.

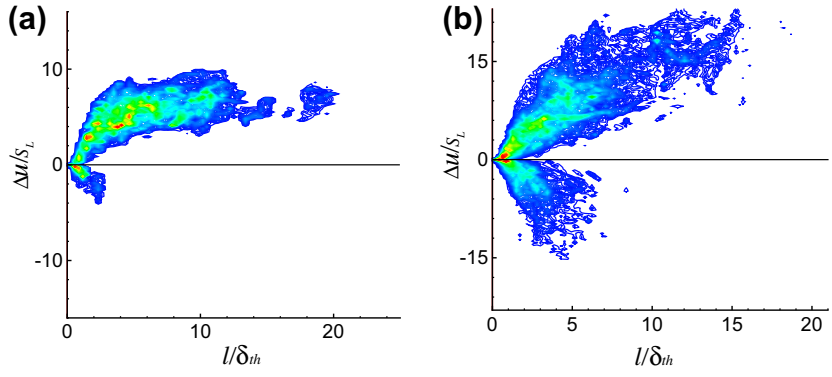

Fig. 9. Same as Fig. 8, but for (a) case D; (b) case H.

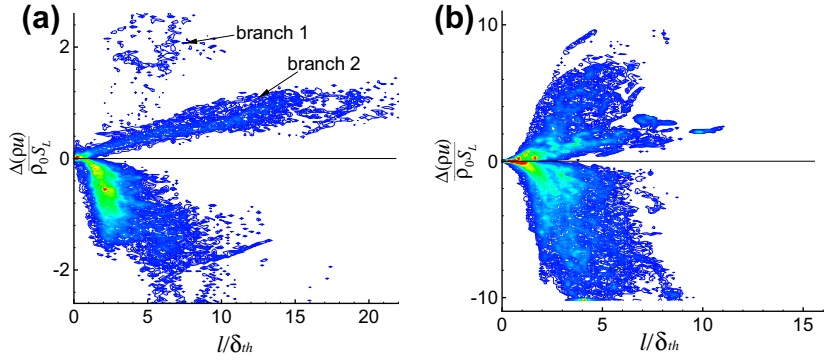

Fig. 10. Joint PDF between l/δ_{th} and $\Delta(\rho u)/\rho_0 S_L$ for (a) case A; (b) case B, based on the streamline segments defined in terms of $\rho\vec{u}$.

branch is much longer in case *B*. In case *A* turbulent motions are largely influenced by thermal expansion, which acts to make the streamline segments passing through flames to be positive, while case *B* resembles to be non-reacting turbulent flow and the joint PDF $P(l, \Delta u)$ shows the attributes of non-reacting flows due to the relatively small value of τ and high value of u'/S_L. The turbulence intensity u'/S_L increases from case *D* to *H* and thus the impact of turbulence becomes increas-

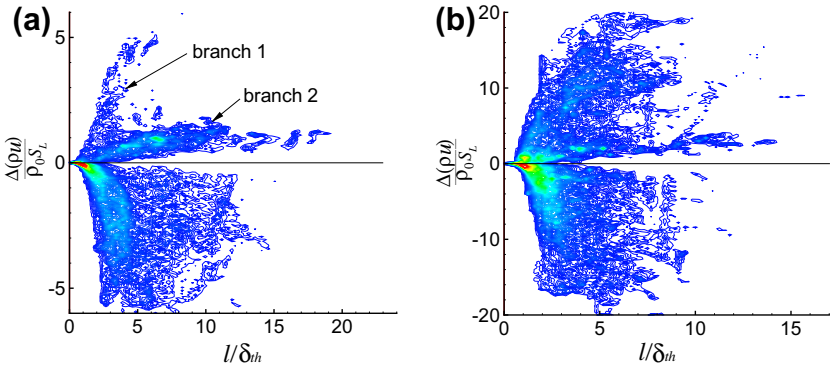

Fig. 11. Same as Fig. 10, but for (a) case D; (b) case H.

ingly strong from cases D to H. As a result of this, the negative Δu part in $P(l,\Delta u)$ increases progressively with increasing u'/S_L, as demonstrated in Fig. 9. Thus, the asymmetry in $P(l,\Delta u)$ can be considered as an indication of the influence of the flame on turbulent motion, i.e. the larger the asymmetry, the stronger the influence of the flame.

An interesting comparison arises from the statistics of the $\rho\vec{u}$ along the streamline segments. The joint PDFs $P(l,\Delta\rho u)$ for cases A and B (cases D and H) are shown in Fig. 10 (Fig. 11), which demonstrate that $P(l,\Delta\rho u)$ is very different from $P(l,\Delta u)$ (see Figs. 8 and 9). In $P(l,\Delta\rho u)$ the part with positive $\Delta\rho u$ shows two branches (i.e. branches 1 and 2) especially for small u'/S_L cases. The interaction between turbulence and flame can be attributed to the effects of thermal expansion and turbulent perturbation. Dilatation rate $\partial u_i/\partial x_i$ due to thermal expansion is a large-scale effect, and ρu does not change significantly across the flame, which in turn gives rise to the long streamline segments with small $\Delta(\rho u)$, accounting for branch 2. By contrast, turbulent motions tend to generate relatively short both positive and negative streamline segments with large magnitude of $\Delta(\rho u)$, which account for branch 1 and the negative $\Delta(\rho u)$ region as well. At small values of u'/S_L and/or large values of τ, thermal expansion plays a dominant role, and thus $P(l,\Delta\rho u)$ for A and D exhibits a prominent branch 2, whereas for high u'/S_L and/or relatively small τ cases (such as B and H), turbulent motion is more important and consequently branch 2 shrinks.

4. Conclusions

Streamline segment analysis has been carried out for turbulent premixed combustion, based on a DNS database of the freely propagating statistically planar unity Lewis number flames with wide variations of τ,Re_t and Ka. The main findings can be summarized as follows:

(1) For small values of u'/S_L the velocity vector remains locally parallel to the flame normal. However, this orientation relation becomes more chaotic with increasing turbulence intensity u'/S_L.
(2) A negative correlation between curvature and Δu is observed for the TRZ cases. The positive and negative streamline segments are likely to push flames to the burned gas side and the unburned gas side, respectively. The CF case shows an opposite tendency.
(3) A PDF distribution of $P(\tilde{l})$, which was derived for non-reacting turbulent flows, remains valid for higher Reynolds number flames in the TRZ regime, but this distribution may not be adequate for small values of Re_t and for the flames in the CF regime.
(4) Relative strengths of dilatation rate and turbulence dynamics ultimately determine the topological features such as $P(l,\Delta u)$ and $P(l,\Delta\rho u)$ in turbulent premixed flames.

In this analysis, the chemical mechanism is simplified using a single step chemistry, and the range of Re_t considered here remains moderate. Thus, three-dimensional DNS data with detailed chemistry at higher values of Re_t will be needed for more comprehensive analysis.

Acknowledgments

L.W. thanks for the funding support by the state key lab of nonlinear mechanics and NSFC (under the Grant No. 11172175). N.C. gratefully acknowledges the financial support of EPSRC, UK.

References

[1] N. Peters, *Turbulent Combustion*, Cambridge University Press, 2000.

[2] I.G. Shepherd, W.T. Ashurst, *Proc. Combust. Inst.* 24 (1992) 485–491, 112(3).
[3] C.K. Law, *Combustion Physics*, *Cambridge University Press* (2006).
[4] T. Echekki, J.H. Chen, *Combust. Flame* 106 (1996) 184–202.
[5] N. Peters, P. Terhoeven, J.H. Chen, T. Echekki, *Proc. Combust. Inst.* 27 (1998) 833–839.
[6] T. Echekki, J.H. Chen, *Combust. Flame* 118 (1999) 303–311.
[7] N. Chakraborty, S. Cant, *Combust. Flame* 137 (2004) 129–147.
[8] N. Chakraborty, R.S. Cant, *Phys. Fluids* 17 (2005) 105105.
[9] M. Klein, N. Chakraborty, K.W. Jenkins, R.S. Cant, *Phys. Fluids* 18 (2006) 055102, 1–15.
[10] N. Chakraborty, *Phys. Fluids* 19 (2007) 105109, 1–20.
[11] N. Chakraborty, M. Klein, R.S. Cant, *J. Combust.* 2011 (2011) 473679.
[12] M. Matalon, B.J. Matkowsky, *J. Fluid Mech.* 124 (1982) 239–259.
[13] N. Chakraborty, R.S. Cant, *Phys. Fluids* 19 (2007) 105101.
[14] N. Chakraborty, R.S. Cant, *Proc. Combust. Inst.* 32 (2009) 1445–1453.
[15] B. Renou, A. Boukhalfa, D. Puechberty, M. Trinite, *Proc. Combust. Inst.* 27 (1998) 841–847.
[16] D.C. Haworth, T.J. Poinsot, *J. Fluid Mech.* 244 (1992) 405–436.
[17] L. Wang, N. Peters, *J. Fluid Mech.* 554 (2006) 457–475.
[18] L. Wang, *J. Fluid Mech.* 648 (2010) 183–203.
[19] A.N. Karpetis, R.S. Barlow, *Proc. Combust. Inst.* 30 (2005) 665–672.
[20] S. Kaiser, J.H. Frank, *Proc. Combust. Inst.* 32 (2009) 1639–1646.
[21] S. Tullis, *Large Eddy Simulation of Scalar Flux in Turbulent Premixed Flames*, Ph.D. thesis, Cambridge Engineering University Department, Cambridge, 2003.
[22] S. Tullis, R.S. Cant, *Proc. Combust. Inst.* 29 (2002) 2097–2104.
[23] J.H. Chen, A. Choudhary, B. de Supinski, et al., *Comput. Sci. Discovery* 2 (2009) 015001.
[24] C.J. Rutland, R.S. Cant, Turbulent transport in premixed flames, in: *Proceedings of 1994 Summer Program, Centre for Turbulence Research*, Stanford University/NASA Ames, Stanford, CA, 1994, pp.75–94.
[25] K.W. Jenkins, R.S. Cant, DNS of turbulent flame kernels, in: D. Knight, L. Sakell (Eds.), Proceedings of Second AFOSR Conference on DNS and LES, Rutgers University, Kluwer Academic Publishers, 1999, pp. 192–202.
[26] H. Kobayashi, T. Kawahata, K. Seyama, T. Fujimari, J. Kim, *Proc. Combust. Inst.* 29 (2002) 1793–1800.
[27] N. Swaminathan, K.N.C. Bray, *Combust. Flame* 143 (2005) 549–565.
[28] F. Charlette, C. Meneveau, D. Veynante, *Combust. Flame* 131 (2002) 181–197.
[29] R.W. Grout, *Phys. Fluids* 19 (2007) 105107.
[30] I. Han, K.H. Huh, *Proc. Combust. Inst.* 32 (2009) 1419–1425.
[31] N. Chakraborty, R.S. Cant, *Combust. Flame* 156 (2009) 1427–1444.
[32] N. Chakraborty, G. Hartung, M. Katragadda, C.F. Kaminski, *Combust. Flame* 158 (2011) 1372–1390.
[33] T. Plessing, C. Kortschik, M.S. Mansour, N. Peters, *Proc. Combust. Inst.* 28 (2000) 359–368.
[34] D. Veynante, A. Trouve, K.N.C. Bray, T. Mantel, *J. Fluid Mech.* 332 (1997) 263–293.
[35] N. Chakraborty, R.S. Cant, *Phys. Fluids* 21 (2009) 035110.